

RESEARCH ARTICLE

# Parametric dependence of collisional heating of highly magnetized over-dense plasma by (far-)infrared lasers

K. Li<sup>1</sup> and W. Yu<sup>2</sup>

<sup>1</sup>Department of Physics, College of Science, Shantou University, Shantou 515063, China

<sup>2</sup>Shanghai Institute of Optics and Fine Mechanics, Chinese Academy of Sciences, Shanghai 201800, China

(Received 6 May 2022; accepted 8 June 2022)

## Abstract

Heating of over-dense plasma represents a long-standing quest in laser–plasma physics. When the strength of the magnetic field is above the critical value, a right-handed circularly polarized laser could propagate into and heat up the highly magnetized over-dense collisional plasma directly; the processes are dependent on the parameters of the laser, plasma and magnetic field. The parametric dependence is fully studied both qualitatively and quantitatively, resulting in scaling laws of the plasma temperature, heating depth and energy conversion efficiency. Such heating is also studied with the most powerful CO<sub>2</sub> and strongest magnetic field in the world, where plasma with density of 10<sup>23</sup> cm<sup>-3</sup> and initial temperature of 1 keV is heated to around 10 keV within a depth of several micrometres. Several novel phenomena are also discovered and discussed, that is, local heating in the region of high density, low temperature or weak magnetic field.

**Keywords:** highly magnetized plasma; over-dense plasma; collisional heating; parametric dependence

## 1. Introduction

The research on inertial confinement fusion (ICF) started as early as 1960s<sup>[1]</sup>, where powerful laser beams should compress the deuterium–tritium (DT) fuel to density over several hundred times of the critical value ( $\sim 10^{21}$  cm<sup>-3</sup>) at a laser wavelength of 1  $\mu$ m and heat the DT fuel up to around 10 keV. Because the non-relativistic laser is unable to propagate into the over-dense plasma due to the permittivity of plasma less than zero, various alternative schemes<sup>[2]</sup> are being pursued, where the intense laser pulses generate electron or ion beams and deposit energy indirectly to the compressed DT fuel, which intrinsically decreases the energy conversion efficiency from the laser to the plasma. However, it has been known for long time that if the electron gyrofrequency of the electromagnetic wave (called laser here) is higher than the laser frequency, that is,  $\omega_c = eB/m_e c > \omega_L$ , the right-handed circularly polarized (RHCP) non-relativistic laser could propagate into the over-dense magnetized plasma<sup>[3–5]</sup>. Such a phenomenon was first studied for the whistler phenomenon of radio waves (wavelength of  $\lambda_L > 10^4$  m) under the conditions of extremely low plasma

density and extremely weak geomagnetic field (magnetic field of  $B_0 < 10^{-4}$  T) in the 1960s<sup>[4]</sup>. With the quick increase of the magnetic field strength in recent years, it is interesting to re-investigate the phenomenon of magnetic-induced plasma transparency, especially in the case of heating highly magnetized over-dense plasma with powerful (far-)infrared lasers propagating inside.

The electron gyrofrequency being higher than the laser frequency is equivalent to the strength of the magnetic field being larger than a critical value,  $B_0 > B_c = 1.07 \times 10^4 \lambda_{L,\mu m}^{-1}$  T<sup>[6,7]</sup>. Under such a condition, the permittivity of the magnetized plasma, in the case of RHCP lasers, is always above unity for any plasma density even above the over-critical value,  $n_e > n_c \approx 1.12 \times 10^{21} \lambda_{L,\mu m}^{-2}$  cm<sup>-3</sup>. For powerful Nd:YAG or CO<sub>2</sub> lasers, which have wavelengths of around 1 or 10  $\mu$ m, the required strength of the magnetic field should be above 10<sup>4</sup> or 10<sup>3</sup> T, respectively. In recent years, researchers have discovered several ways to generate the macroscopic magnetic field with strength close to or higher than 10<sup>3</sup> T in experiments. For example, in the scheme of a laser-driven capacitor-coil, a quasistationary magnetic field up to 600 T was generated when the Nd:glass laser with duration of 1 ns, pulse energy of 500 J and intensity of 10<sup>17</sup> W cm<sup>-2</sup> was focused onto a copper coil with a coil

Correspondence to: K. Li, Department of Physics, College of Science, Shantou University, Shantou 515063, China. Email: [kunli@stu.edu.cn](mailto:kunli@stu.edu.cn)

diameter of 500  $\mu\text{m}$  and wire cross-section of 50  $\mu\text{m}$ <sup>[8,9]</sup>. In the scheme of magnetic field compression by electromagnetic flux, the seed magnetic field of 3.2 T is enhanced to as high as 1200 T with input current energy of around 3 MJ<sup>[10]</sup>. Such compression is also achieved using powerful OMEGA laser beams with energy of several kilojoules<sup>[11]</sup>, then the seed magnetic field is increased to the world-record 4000 T inside the cylindrically compressed deuterium plasma, where the averaged plasma density is around  $10^{23} \text{ cm}^{-3}$ , and the plasma temperature is around 3 keV at the cylindrical axis and around 0.5 keV at the radius of 15  $\mu\text{m}$ . In theory, a longitudinal magnetic field even as high as  $10^6$  T is obtained in the scheme of intense laser-driven micro-tube implosions, but with a microscopic dimension smaller than 1  $\mu\text{m}$ <sup>[12]</sup>.

The collisional interaction of RHCP lasers with highly magnetized over-dense plasma has been studied by the authors previously. In the first paper<sup>[6]</sup>, the propagation of an RHCP laser from vacuum into highly magnetized over-dense plasma is studied, where the plasma temperature is assumed to be constant. In the second paper<sup>[7]</sup>, the process of collisional heating is studied and the plasma is heated from 0.1 keV to around 1 keV, with other parameters of the laser, plasma and magnetic field being fixed. In this paper, the parameter dependence of this process will be studied both qualitatively and quantitatively, the scaling laws of plasma temperature, averaged heating depth and energy conversion efficiency will be obtained, and then plasma heating under more ‘practical’ conditions will be investigated.

## 2. Parameter dependence of plasma heating

The permittivity of magnetized collisional plasma, in the case of an RHCP wave, is given in the previous work<sup>[6,7]</sup>:

$$\varepsilon = 1 + \frac{n}{B - 1 - i\nu}, \quad (1)$$

where  $n = n_e/n_c$  is the dimensionless plasma density with  $n_c \approx 1.12 \times 10^{21} \lambda_{L,\mu\text{m}}^{-2} \text{ cm}^{-3}$ ,  $B = B_0/B_c$  is the dimensionless magnetic field with  $B_c = 1.07 \times 10^4 \lambda_{L,\mu\text{m}}^{-1} \text{ T}$  and  $\nu = \nu_{ei}/\omega_L \approx 1.72 (\ln \Lambda) Z n \lambda_L^{-1} T_{\text{eV}}^{-3/2}$  is the dimensionless electron-ion collision rate<sup>[13]</sup>, with  $\omega_L$  being the angular frequency of the laser,  $Z$  is the number of free electrons per atom,  $T_{\text{eV}}$  is the plasma temperature in unit of electron-volts,  $\lambda_L$  is the wavelength of the laser in unit of micrometres and  $\ln \Lambda$  is the Coulomb logarithm. The complex refractive index of plasma is  $\tilde{n} = n_r + in_i = \sqrt{\varepsilon}$ , and thus  $n_r$  is always positive in the case  $B > 1$  and the RHCP laser could propagate into plasma with any high density and deposit energy. The dependence of plasma heating on the parameters of the laser, plasma and magnetic field will be studied both qualitatively and quantitatively.

### 2.1. Qualitative investigation

In this paper, plasma or gas of deuterium and tritium will be studied, and thus  $Z$  is equal to 1 and  $\ln \Lambda$  is assumed to be 1. The basic parameters in this paper are similar to previous work<sup>[6,7]</sup>, that is,  $\lambda_L = 1 \mu\text{m}$ ,  $n_e = 10^{23} \text{ cm}^{-3}$  ( $n = 100$ ),  $B_0 = 10^5 \text{ T}$  ( $B = 10$ ), and the initial plasma temperature is  $T_0 = 0.1 \text{ keV}$ , showing that the dimensionless collision rate is much less than unity, that is,  $\nu \ll 1$ . In this way, the dimensionless wave vector of the RHCP laser inside the plasma can be approximated as follows under conditions of  $\nu \ll 1$  and  $B > 1$ :

$$k = \sqrt{\varepsilon} = k_r + ik_i \approx \left(1 + \frac{n}{B-1}\right)^{1/2} + \frac{i}{2} \frac{n\nu}{(B-1)^2} \left(\frac{1}{1+n/(B-1)}\right)^{1/2}, \quad (2)$$

where  $k$  is the dimensionless wave vector of the RHCP laser in plasma, equalling the complex refractive index of plasma, that is,  $k = \tilde{n}$  and  $n_r + in_i = k_r + ik_i$ . The dimensionless wave vector is further approximated in the region of  $n \gg B \gg 1$  with the effect of plasma temperature and laser wavelength:

$$k_L = k_r + ik_i \approx \left(\frac{n_1}{B_1} \cdot \frac{\lambda_L}{\lambda_1}\right)^{1/2} + i \cdot 0.86 (\ln \Lambda) Z \left(\frac{n_1}{B_1 T_{\text{eV}}}\right)^{3/2} \frac{\lambda_L^{1/2}}{\lambda_1^{3/2}}, \quad (3)$$

where the parameters of the laser, plasma and magnetic field at a wavelength of 1  $\mu\text{m}$  are denoted by subscript ‘1’ and  $k_L$  is the dimensionless wave vector at wavelength  $\lambda_L$ . It is also found that laser is blue-shifted inside the plasma since  $k_r$  is always above unity, and at the same time, the wavelength of laser inside the plasma decreases with higher plasma density and weaker magnetic field. The power transmission of the normally incident laser from vacuum into plasma and its approximation under the condition of  $n \gg B \gg 1$  are obtained based on the Fresnel equations:

$$\text{Trans.} = \frac{4k_r}{(1+k_r)^2} \approx 4 \left(\frac{B}{n}\right)^{1/2} = 4 \left(\frac{B_1}{n_1} \cdot \frac{\lambda_1}{\lambda_L}\right)^{1/2}. \quad (4)$$

In this way, the power transmission increases with lower plasma density, higher magnetic field and shorter laser wavelength, while it is not sensitive to plasma temperature, laser intensity and heating duration. For example,  $\text{Trans.} \approx 0.3$  for  $B = 2$  and  $n = 100$ , while  $\text{Trans.} \approx 0.7$  for  $B = 10$  and  $n = 100$ , showing that  $B > 3$  is required for high-power transmission. The attenuation length at wavelength  $\lambda_L$  in

practical unit becomes

$$L_{\alpha, \lambda_L} = (2k_L k_i)^{-1} \approx 0.1 (\ln \Lambda)^{-1} Z^{-1} \lambda_1^{3/2} \lambda_L^{1/2} \left( \frac{B_1 T_{eV}}{n_1} \right)^{3/2}. \quad (5)$$

In this way, the absorption length increases with lower plasma density, higher plasma temperature (thus laser intensity and duration), higher magnetic field and larger laser wavelength, which means that the RHCP laser prefers to deposit energy locally in the region of a weaker magnetic field, lower plasma temperature and higher plasma density. The increase of attenuation length with larger laser wavelength seems counter-intuitive, and thus it is further studied by varying the laser wavelength while keeping other parameters constant, for example,  $B_0 = 10^5$  T,  $n_e = 10^{23}$  cm<sup>-3</sup> and  $T = 100$  eV. It is found that when  $\lambda_L < 0.1$  μm (in the region of  $B < 1$ ), the attenuation length increases with shorter laser wavelength; however, when  $\lambda_L > 0.1$  μm (in the region of  $B > 1$ ), the attenuation length indeed increases with larger laser wavelength. In this way, in the region of  $B > 1$ , a laser with larger wavelength propagates deeper in the highly magnetized over-dense plasma.

### 2.2. Quantitative investigation

The quantitative dependence is obtained by solving the equation of energy conservation between the laser and plasma as in the previous work<sup>[7]</sup>, which is based on the processes of laser transmission and collisional absorption. The dimensionless potential vector of an incident planar RHCP laser propagating in vacuum is expressed as  $\mathbf{a} = a_0 e^{i\mathbf{k}\cdot\mathbf{r} - t} (\vec{x} + i\vec{y})$ , where  $t = \omega_L t_0$  is the dimensionless time,  $z = k_L z_0$  is the dimensionless space and  $I_L \lambda_{L, \mu m}^2 \approx 1.37 \times 10^{18} a_0^2$  W cm<sup>-2</sup> with  $a_0 \approx 0.01$  for  $I_L = 10^{14}$  W cm<sup>-2</sup> and  $\lambda_L = 1$  μm. For a normally incident laser, the dimensionless potential vector of the laser in plasma becomes

$$\mathbf{a}_1 = t \cdot a_0 \cdot e^{i\mathbf{k}\cdot\mathbf{r} - t} (\vec{x} + i\vec{y}), \quad (6)$$

where  $k$  is the dimensionless wave vector in Equation (2) and  $t = 2/(1+k)$  is the transmission coefficient for the potential vector of the laser from vacuum to plasma. In the process of collisional interaction, the transverse velocity of electron driven by the RHCP laser in the magnetized plasma is as follows:

$$\mathbf{u}_t = \frac{\mathbf{a}_1}{1 - B + i\nu}. \quad (7)$$

Thus, the rate of laser absorption in plasma is  $\nabla \cdot \mathbf{S}_t = \partial_z (a_1 a_1^*)$ , and the rate of plasma heating by transverse electron current is the imaginary part of  $-\mathbf{J}_t \cdot \mathbf{E}_t = -n u_t \cdot a_1$ . The equation of plasma heating is thus obtained based on

energy conservation between the laser and plasma:

$$\partial_t (w_P + w_L) = -\nabla \cdot \mathbf{S}_t - \text{Im}(\mathbf{J}_t \cdot \mathbf{E}_t), \quad (8)$$

where  $w_L = (1 + \text{Re}(\epsilon)) a^2/2$  is the dimensionless energy density of the laser propagating inside plasma and  $w_P$  is the dimensionless energy density of plasma. In this paper, only the ideal gas-like plasma will be studied, requiring the plasma temperature to be much higher than the Fermi temperature,  $T_{eV} > \epsilon_F \approx 7.9 n_{23}^{2/3}$  eV. In this case, the dimensionless energy density of plasma is expressed as  $w_P = 3nT^{[14]}$ , with  $T = T_{eV}/m_e c^2$  being the dimensionless plasma temperature. It should be noted that the energy loss of cyclotron emission is not taken into account here, and thus this equation is valid only when the strength of the magnetic field is much smaller than  $10^5$  T, which will be explained later in this paper.

Equation (8) is solved with the plasma temperature shown as the two identical black curves in Figures 1(a) and 1(b) with the set of basic parameters  $\tau_L = 1$  ns,  $\lambda_L = 1$  μm,  $a_0 = 0.01$ ,  $n = 100$ ,  $T_0 = 100$  eV and  $B = 10$ , which could be translated into practical units as  $I_L \approx 10^{14}$  W/cm<sup>2</sup>,  $n_e \approx 10^{23}$  cm<sup>-3</sup> and  $B_0 \approx 10^5$  T. When only one of above parameters is changed, the modified plasma temperature is shown as the colourful curves in Figures 1(a) and 1(b). It should be noted that the solid red curve in Figure 1(a) is shown at 10 ns while all others are at 1 ns. In this way, the dependences of plasma temperature at the vacuum–plasma boundary and averaged heating depth (attenuation length) on the parameters of the laser, plasma and magnetic field are obtained and are listed in Table 1, where the upper arrow means ‘increase with’, down arrow means ‘decrease with’ and the right arrow means ‘not sensitive to’. The dependence of power transmission is also calculated based on Equation (8) and is given in Table 1, which is not sensitive to an initial temperature above 100 eV because the dimensionless collisional rate is already much smaller than 1 for temperatures above 100 eV. The tendencies are same for the qualitative results.

### 2.3. Scaling laws

The scaling law can be obtained but only within the restricted region of parameters. For the set of basic parameters,  $\lambda_L = 1$  μm,  $I_L = 10^{14}$  W cm<sup>-2</sup>,  $n_e = 10^{23}$  cm<sup>-3</sup> and  $B_0 = 10^5$  T, the scaling law of the averaged heating depth scales versus the initial plasma temperature ( $T_0$ ) is approximately to be

$$d_{\mu m} \approx 120 \cdot T_0(\text{keV})^{0.93}. \quad (9)$$

while the boundary plasma temperature ( $T_b$ ) is not sensitive to  $T_0$ . In this way, the RHCP laser could heat the hotter over-dense plasma in larger deepness. For fixed initial plasma temperature of  $T_0 = 0.1$  keV, the scaling law of the bound-

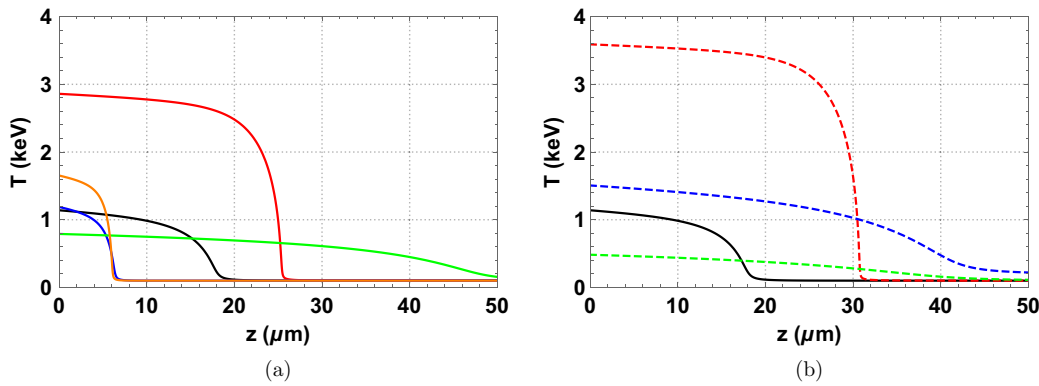


**Figure 1.** The temperature of plasma versus laser propagation depth inside plasma for the incident planar flat-top RHCP laser with duration of 1 ns except for the red solid curve of 10 ns. Parameters of the two identical black curves in (a) and (b): laser wavelength of  $\lambda_L = 1 \mu\text{m}$ , intensity of  $I_L = 10^{14} \text{ W/cm}^2$ , duration of  $\tau_L = 1 \text{ ns}$ , plasma density of  $n_e = 10^{23} \text{ cm}^{-3}$ , initial plasma temperature of  $T_0 = 0.1 \text{ keV}$  and magnetic field of  $B_0 = 10^5 \text{ T}$ . Each of the other six colourful curves has one of the above parameters being changed, that is, (a)  $\tau_L = 10 \text{ ns}$  (red, solid),  $n_e = 2 \times 10^{23} \text{ cm}^{-3}$  (blue, solid),  $B_0 = 2 \times 10^5 \text{ T}$  (green, solid) and  $B_0 = 0.5 \times 10^5 \text{ T}$  (orange, solid); (b)  $I_L = 10^{15} \text{ W/cm}^2$  (red, dotted),  $T_0 = 200 \text{ eV}$  (blue, dotted) and  $\lambda_L = 10 \mu\text{m}$  (green, dotted).

**Table 1.** Power transmission of the laser (Trans.), increase of plasma temperature at the vacuum–plasma boundary ( $T_b - T_0$ ), averaged heating depth in micrometres ( $d_{\mu\text{m}}$ ) and energy conversion efficiency from laser to plasma ( $\eta_{L \rightarrow P}$ ) versus various parameters, where  $\uparrow$  means ‘increase with’,  $\downarrow$  means ‘decrease with’ and  $\rightarrow$  means ‘not sensitive to’.

	$n_e$	$T_0$	$B_0$	$I_L$	$\tau_L$	$\lambda_L$
Trans.	$\downarrow$	$\rightarrow$	$\uparrow$	$\rightarrow$	$\rightarrow$	$\uparrow$
$T_b - T_0$	$\uparrow$	$\downarrow$	$\downarrow$	$\uparrow$	$\uparrow$	$\downarrow$
$d_{\mu\text{m}}$	$\downarrow$	$\uparrow$	$\uparrow$	$\uparrow$	$\uparrow$	$\uparrow$
$\eta_{L \rightarrow P}$	$\downarrow$	$\rightarrow$	$\uparrow$	$\downarrow$	$\downarrow$	$\downarrow$

ary plasma temperature versus the parameters of the laser, plasma and magnetic field is as follows:

$$T_{b, \text{keV}} \approx 1.15 \cdot (I_{14} \cdot \tau_{\text{ns}})^{0.4} \cdot (B_0/10^5)^{-0.55} \cdot \lambda_{\mu\text{m}}^{-0.75}, \quad (10)$$

and the scaling law of averaged heating depth is as follows:

$$d_{\mu\text{m}} \approx (15 + 7.7 \log(I_{14} \cdot t_{\text{ns}}) + 10 \log(\lambda_{\mu\text{m}})) \cdot (B_0/10^5)^{1.37} \cdot n_{23}^{-1.53}, \quad (11)$$

where  $d_{\mu\text{m}}$  is the averaged heating depth in micrometres,  $T_{b, \text{keV}}$  is the boundary temperature in keV,  $t_{\text{ns}}$  is the heating duration in nanoseconds,  $I_{14}$  is the laser intensity in  $10^{14} \text{ W cm}^{-2}$ ,  $\lambda_{\mu\text{m}}$  is the wavelength of the incident laser in micrometres,  $B_0$  is the strength of the magnetic field in teslas,  $n_{23}$  is the plasma density in units of  $10^{23} \text{ cm}^{-3}$ . The above two scaling laws work under conditions of  $B > 3$ ,  $t > 0.01 \text{ ns}$ ,  $I_L > 10^{12} \text{ W cm}^{-2}$  and  $0.1 < \lambda_L < 20 \mu\text{m}$ . It is found that both the boundary temperature and heating depth increase with the radiant exposure ( $\text{J/cm}^2$ ), the heating depth is most sensitive to the strength of the magnetic field and plasma density, and the boundary plasma temperature is most sensitive to the strength of the magnetic field and laser wavelength. In this way, a laser with larger wavelength should be applied to increase the heating depth, although with the sacrifice of decreased plasma temperature.

The energy conversion efficiency from the laser to plasma is as follows:

$$\eta_{L \rightarrow P} = \frac{W_p}{W_L} = \left( \int_0^{z_{\text{max}}} 3n_e \Delta T dz \right) \cdot (I_L \tau)^{-1} \approx 0.048 n_{23} \frac{(T_{b, \text{keV}} - T_{0, \text{keV}}) d_{\mu\text{m}}}{I_{14} \tau_{\text{ns}}}. \quad (12)$$

Inserting Equations (10) and (11), the energy conversion efficiency becomes

$$\eta_{L \rightarrow P} \approx 0.055 \cdot (B_0/10^5)^{0.82} \cdot \frac{15 + 3.33 \log(I_{14} \tau_{\text{ns}}) + 10 \log(\lambda_{\mu\text{m}})}{(I_{14} \tau_{\text{ns}})^{0.6} n_{23}^{0.53} \lambda_{\mu\text{m}}^{0.75}}. \quad (13)$$

In this way, the conversion efficiency increases with strength of the magnetic field, while it decreases with the radiation exposure of the laser, plasma density and wavelength of the laser, which is shown in Table 1. It should be noted again that since Equation (8) is valid when  $B_0 \ll 10^5 \text{ T}$ , the above scaling laws also work only in this region.

### 3. Plasma heating with a powerful CO<sub>2</sub> laser

Because the maximum available longitudinal macroscopic magnetic field is around  $4 \times 10^3 \text{ T}^{[11]}$ , a powerful laser with wavelength longer than  $2.5 \mu\text{m}$  must be found for ‘practical’

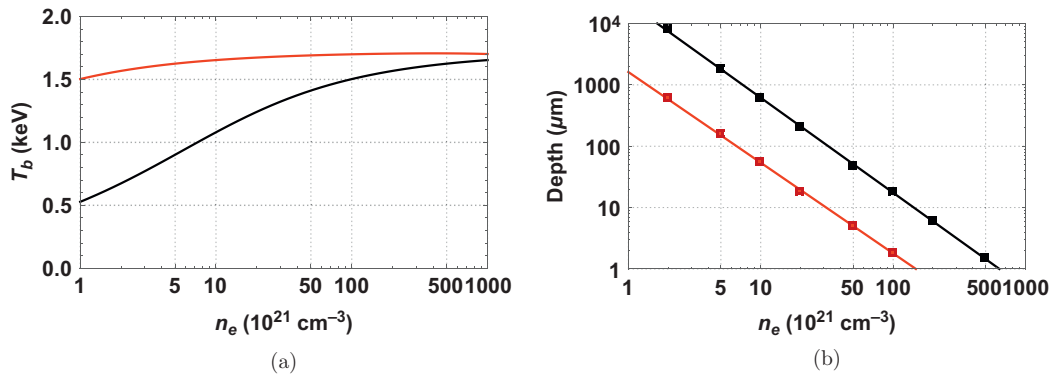


**Figure 2.** Heating of plasma with different densities by CO<sub>2</sub> laser and Nd:YAG laser with  $I_L = 10^{14} \text{ W cm}^{-2}$ ,  $\tau_L = 1 \text{ ns}$  and  $T_0 = 0.1 \text{ keV}$ . (a) Plasma temperature at the vacuum–plasma boundary versus plasma density:  $\lambda_L = 1 \text{ } \mu\text{m}$ ,  $B_0 = 10^5 \text{ T}$  (black) and  $\lambda_L = 10 \text{ } \mu\text{m}$ ,  $B_0 = 10^4 \text{ T}$  (red). (b) Averaged heating depth versus plasma density:  $\lambda_L = 1 \text{ } \mu\text{m}$ ,  $B_0 = 10^5 \text{ T}$  (black) and  $\lambda_L = 10 \text{ } \mu\text{m}$ ,  $B_0 = 10^4 \text{ T}$  (red), where the dots denote simulated depth and the lines denote the fitted curve.

heating of plasma with density above  $10^{21} \text{ cm}^{-3}$ , which is of interest in the field of laser–plasma-interaction. At the Brookhaven National Laboratory (BNL)<sup>[15]</sup>, a CO<sub>2</sub> laser at the wavelength of  $9.4 \text{ } \mu\text{m}$  is being built with pulse duration of 100 ps and pulse energy of around 70 J, which translates to a maximum laser intensity of around  $7 \times 10^{17} \text{ W cm}^{-2}$  at a focal spot diameter of  $10 \text{ } \mu\text{m}$ . To the best of the authors’ knowledge, this is the most powerful laser with a wavelength above  $2.5 \text{ } \mu\text{m}$  right now.

In this way, over-dense plasma heating by a CO<sub>2</sub> laser at a wavelength of  $10 \text{ } \mu\text{m}$  and magnetic fields of  $4 \times 10^3$  and  $10^4 \text{ T}$  will be studied and compared with a Nd : YAG laser, as shown in Figures 2(a) and 2(b), respectively. The dimensionless magnetic field is chosen to be  $B = 10$  for both cases, which is translated into  $B_0 = 10^4 \text{ T}$  for the CO<sub>2</sub> laser and  $B_0 = 10^5 \text{ T}$  for the Nd : YAG laser. In both cases, the laser intensity is  $10^{14} \text{ W cm}^{-2}$ , the duration is 1 ns and the initial plasma temperature is 0.1 keV. The averaged heating depth is simulated at various plasma densities, shown as red dots and fitted with a curve that has the same scaling law as Equation (11). It is found that plasma with lower density in the range of  $10^{21}$ – $10^{22} \text{ cm}^{-3}$  could be heated up to 0.1–1 keV within depth 10–100  $\mu\text{m}$ . For the realized magnetized plasma with  $B_0 = 4 \times 10^3 \text{ T}$ ,  $n_e = 10^{23} \text{ cm}^{-3}$  and  $T_0 = 1 \text{ keV}$  (assumed uniform)<sup>[11]</sup>, if the 1-ns CO<sub>2</sub> laser pulse is focused to an intensity of  $10^{14}$  or  $10^{16} \text{ W cm}^{-2}$ , the plasma temperature will increase from 1 to 3 keV within several micrometres, as shown in Figure 3(a).

The properties of local heating or heating of non-uniform over-dense plasma are studied with sandwiched targets, as shown in Figure 3(b), where the plasma densities are  $10^{22} \text{ cm}^{-3}$  in the first and third layers and  $10^{23}$  or  $5 \times 10^{23} \text{ cm}^{-3}$  in the second layer. It is found that the CO<sub>2</sub> laser indeed deposits energy in the region of higher plasma density. The tendency of energy deposition in the region of lower temperature and weaker magnetic field is similar but not shown here.

#### 4. Discussion and conclusions

The energy loss of cyclotron emission will be discussed here, especially for the plasma heating with a CO<sub>2</sub> laser at a magnetic field of  $B_0 = 10^4 \text{ T}$ . In this case, the frequency of cyclotron emission is around  $f_c \approx 2.8 \times 10^{10} B(T) = 2.8 \times 10^{14} \text{ Hz}$ , smaller than the critical plasma frequency of  $2.8 \times 10^{15} \text{ Hz}$ , and thus the plasma is opaque to the cyclotron emission. The energy of cyclotron emission per volume is approximated to be  $6.21 B_{\text{KT}}^2 n_{23} T_{\text{keV}} \tau_{\text{ns}} (\text{J/mm}^3)$ <sup>[16]</sup> while the energy density of plasma is  $4.8 \times 10^4 n_{23} T_{\text{keV}} (\text{J/mm}^3)$ , and thus their ratio is approximately  $1.3 \times 10^{-4} B_{\text{KT}}^2 \tau_{\text{ns}}$ , which is as small as 0.013 in the case of  $B_0 = 10^4 \text{ T}$  and  $\tau_L = 1 \text{ ns}$ . In this way, the red curves in Figure 2, the curves in Figure 3 and the scaling laws are valid under condition of  $B_0 \leq 10^4 \text{ T}$ . The contribution of cyclotron emission will be discussed in the future.

The energy density and pressure in the high-energy density plasma and magnetic field are very high here, for example, in the case of  $B_0 = 10^4 \text{ T}$ ,  $n_e = 10^{23} \text{ cm}^{-3}$  and  $T_e = 1 \text{ keV}$ . The energy density and pressure of the magnetic field are approximately  $w_B \approx 400 B_{\text{KT}}^2 = 4 \times 10^4 \text{ J/mm}^3$  and  $P_B \approx 400 \text{ Mbar}$ , and the energy density and pressure of plasma are  $w_P \approx 4.8 \times 10^4 n_{23} T_{\text{keV}} = 4.8 \times 10^4 \text{ J/mm}^3$  and  $P_P \approx 480 \text{ Mbar}$ . Because the ion sound velocity is approximately  $c_s \approx 300 T_{\text{keV}}^{1/2} \text{ } \mu\text{m/ns}$ <sup>[16]</sup> in our case, the plasma would disassemble in a very short time, that is, a fraction of 1 ns, if not well confined. In order to confine the heated plasma, the strong CO<sub>2</sub> laser should be coupled to setups with high compression pressure, for example in the scheme of strong magnetic field generation<sup>[11]</sup> or magnetized linear inertial fusion (MagLIF)<sup>[17,18]</sup>. In MagLIF, the axial magnetic field is used to limit the thermal conduction from the hot plasma to the cold linear walls during the implosion, while in this paper the magnetic field will further assist in the increase of plasma temperature. Furthermore, although the energy densities of the magnetic field and plasma are

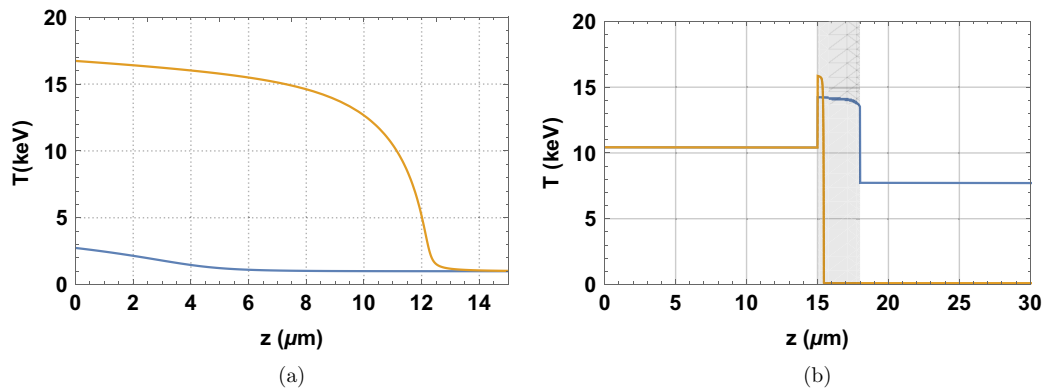


**Figure 3.** Heating of various plasmas by CO<sub>2</sub> laser. (a) The uniform plasma is similar to the compressed plasma in Gotchev *et al.*<sup>[11]</sup>, with  $I_L = 10^{14} \text{ W cm}^{-2}$  (blue) or  $I_L = 10^{16} \text{ W cm}^{-2}$  (orange),  $\tau_L = 1 \text{ ns}$ ,  $B_0 = 4 \times 10^3 \text{ T}$  and  $T_0 = 1 \text{ keV}$ . (b) Sandwiched target with plasma densities of  $n_e = 10^{22} \text{ cm}^{-3}$  ( $0 < z < 15 \mu\text{m}$  and  $z > 18 \mu\text{m}$ ) and  $n_e = 10^{23} \text{ cm}^{-3}$  (blue) or  $n_e = 5 \times 10^{23} \text{ cm}^{-3}$  (yellow) ( $15 \mu\text{m} < z < 18 \mu\text{m}$ ), where  $I_L = 10^{16} \text{ W cm}^{-2}$ ,  $\tau_L = 1 \text{ ns}$ ,  $T_0 = 0.1 \text{ keV}$  and  $B_0 = 10^4 \text{ T}$ .

similar here, the energy conversion efficiency in the generation of a strong magnetic field by laser compression (the energy of the compression lasers is around  $10 \text{ kJ}$ <sup>[11]</sup>) is much less than by plasma heating. In this way, investigation of the efficient generation of a strong magnetic field is required to improve the total energy conversion efficiency.

Plasma heating with more ‘practical’ magnetic fields<sup>[19]</sup> of 100 and 10 T is discussed here. (1) When  $B_0 = 100 \text{ T}$ , lasers with wavelength larger than  $100 \mu\text{m}$  are required to satisfy the condition of  $B > 1$  in the heating plasma with density above  $10^{21} \text{ cm}^{-3}$ . Here, the heating of low-density foam at room temperature is studied as to the possibility for the generation of warm dense matter. For example, conditions of  $n_e = 2 \times 10^{21} \text{ cm}^{-3}$ ,  $T_0 = 0.026 \text{ eV}$  (300 K),  $\lambda_L = 300 \mu\text{m}$  (or 1 THz),  $I_L = 10^{10} \text{ W cm}^{-2}$ ,  $\tau_L = 0.1 \text{ ns}$  and  $B_0 = 100 \text{ T}$  are applied, which results in plasma temperature between 0.125 eV (Fermi energy) and 4.2 eV within a depth of around  $15 \mu\text{m}$ . The energy of this terahertz pulse is 0.9 mJ for the beam diameter of  $300 \mu\text{m}$ , while a terahertz pulse with energy of 0.9 mJ has been efficiently generated from an organic DSTMS (4-N,N-dimethylamino-4’-N’-methyl-stilbazolium 2,4,6-trimethylbenzenesulfonate) crystal by a short-pulsed laser<sup>[20]</sup>. It must be noted that the initial temperature of 0.026 eV is below the Fermi energy, and thus the energy density of ‘plasma’ in Equation (8) should be modified, which requires further investigation. (2) When  $B_0 = 10 \text{ T}$ , lasers with a wavelength larger than  $1000 \mu\text{m}$  are required to heat the over-dense plasma, but the heating depth, boundary plasma temperature and energy conversion efficiency become too small to be applicable, as shown in the scaling laws. It might find applications in heating plasma with density below  $10^{21} \text{ cm}^{-3}$  but is still over-dense for the  $1000\text{-}\mu\text{m}$  ‘laser’, such as in the scheme of magnetic fusion, but not in the scope of this paper. In addition, Equation (8) is still valid for both RHCP and left-handed circularly polarized (LHCP) lasers in the region of

$B < 1$  and  $n < 1$ , and thus it could also be used in applications such as magnetic field measurement due to the Faraday effect or magnetic splitting of a short-pulse laser in plasma<sup>[21]</sup> if the plasma heating by the probe laser is to be necessarily taken into account.

The analytical study in this paper has clarified the main properties of plasma heating but is still very preliminary. For example, collisional heating might not be the only process of laser–plasma interaction in the intensity range of  $10^{14}$ – $10^{16} \text{ cm}^{-2}$  for CO<sub>2</sub> lasers and at this high plasma density level; thus, the simplified calculation here is used to explain the basic heating results due to the phenomenon of magnetically-induced transparency. The effect of a non-uniform magnetic field is not discussed here. For example, the magnetic profile with a strong field at the centre and a weak one at the edge<sup>[11]</sup> will generate magnetized plasma with a refractive index as the negative lens, which will defocus the laser. In addition, non-uniform plasma with a higher density at the centre will work as a positive lens. These effects will be discussed in the future work. Furthermore, only a transverse mode laser is taken into account, while the longitudinal mode also exists in the over-dense magnetized plasma, which will also be discussed in the future.

In conclusion, the collisional heating of highly magnetized over-dense plasma by an RHCP laser is completely studied here with novel phenomena discovered, for example, the laser is blue-shifted in the over-dense plasma, the heating depth increases with larger wavelength in the region of  $B > 1$  and the laser deposits energy locally due to a higher density, lower temperature or weaker magnetic field. The scaling laws are obtained, and thus the dependence of plasma heating on the parameters of the laser, plasma and magnetic field is quantitatively clarified, and the scaling law could be applied in guiding possible applications in the future. Plasma heating with a nanosecond CO<sub>2</sub> laser at the intensity of  $10^{16} \text{ cm}^{-2}$  and magnetic field of  $4 \times 10^3 \text{ T}$  is studied, and if well confined, the DT plasma with density of  $10^{23} \text{ cm}^{-3}$  and

initial temperature of 1 keV could be heated to nearly 10 keV within around 10  $\mu\text{m}$ .

### Acknowledgements

The authors gratefully acknowledge the discussion with Professor Vladimir Tikhonchuk of Centre Lasers Intenses et Applications and University of Bordeaux and Prof. Xu Han of the National University of Defense Technology. This work was supported by the Start-up fund from Shantou University (No. NTF21003), the Science and Technology Fund of Guangdong Province (No. STKJ2021018) and the National Natural Science Foundation of China (NSFC) (No. 12075317).

### Data availability

The data that support the findings of this study are available from the corresponding author upon reasonable request.

### References

1. S. Atzeni and J. Meyer-ter Vehn, *The Physics of Inertial Fusion: Beam-Plasma Interaction, Hydrodynamics, Hot Dense Matter* (Oxford University Press, Oxford, 2004).
2. M. Tabak, P. Norreys, V. Tikhonchuk, and K. Tanaka, *Nucl. Fusion* **54**, 54001 (2014).
3. V. L. Ginzburg, *The Propagation of Electromagnetic Waves in Plasmas* (Pergamon, Oxford, 1970).
4. F. F. Chen, *Introduction to Plasma Physics and Controlled Fusion* (Springer, New York, 2013).
5. T. Boyd and J. Sanderson, *The Physics of Plasmas* (Cambridge University Press, New York, 2003).
6. K. Li and W. Yu, *Phys. Plasmas* **26**, 092106 (2019).
7. K. Li and W. Yu, *Phys. Plasmas* **27**, 102712 (2020).
8. J. Santos, M. Bailly-Grandvaux, L. Giuffrida, P. Forestier-Colleoni, S. Fujioka, Z. Zhang, P. Korneev, R. Bouillaud, S. Dorard, D. Batani, M. Chevrot, J. E. Cross, R. Crowston, J.-L. Dubois, J. Gazave, G. Gregori, E. d'Humières, S. Hulin, K. Ishihara, S. Kojima, E. Loyez, J.-R. Marquès, A. Morace, P. Nicolaï, O. Peyrusse, A. Poyé, D. Raffestin, J. Ribolzi, M. Roth, G. Schaumann, F. Serres, V. T. Tikhonchuk, P. Vacar, and N. Woolsey, *New J. Phys.* **17**, 083051 (2015).
9. V. Tikhonchuk, M. Bailly-Grandvaux, J. Santos, and A. Poye, *Phys. Rev. E* **96**, 023202 (2017).
10. D. Nakamura, A. Ikeda, H. Sawabe, Y. Matsuda, and S. Takeyama, *Rev. Sci. Instrum.* **89**, 095106 (2018).
11. O. Gotchev, P. Chang, J. Knauer, D. Meyerhofer, O. Polomarov, J. Frenje, C. Li, M.-E. Manuel, R. Petrasso, J. Rygg, F. H. Séguin, and R. Betti, *Phys. Rev. Lett.* **103**, 215004 (2009).
12. M. Murakami, J. Honrubia, K. Weichman, A. Arefiev, and S. Bulanov, *Sci. Rep.* **10**, 16653 (2020).
13. W. Kruer, *The Physics of Laser Plasma Interactions* (CRC Press, Boca Raton, FL, 2003).
14. R. P. Drake, *High energy density physics: Fundamentals, Inertial Fusion and Experimental Astrophysics* (Springer, New York, 2006).
15. I. V. Pogorelsky, M. Babzien, I. Ben-Zvi, J. Skaritka, and M. N. Polyanskiy, *Nucl. Instrum. Methods Phys. Res. Sect. A* **829**, 432 (2016).
16. J. D. Huba, *NRL Plasma Formulary* (Plasma Physics Division, Naval Research Laboratory, Washington, DC, 2006).
17. D. Sinars, *Magnetized Liner Inertial Fusion (MagLIF) Research at Sandia National Laboratories* (Sandia National Laboratory (SNL-NM), Albuquerque, NM, 2015).
18. D. Yager-Elorriaga, M. R. Gomez, D. E. Ruiz, S. A. Slutz, A. J. Harvey-Thompson, C. Jennings, P. Knapp, P. Schmit, M. Weis, T. J. Awe, G. A. Chandler, M. A. Mangan, C. E. Myers, J. R. Fein, B. R. Galloway, M. Geissel, M. E. Glinsky, S. B. Hansen, E. C. Harding, D. C. Lamppa, W. E. Lewis, P. Rambo, G. K. Robertson, M. E. Savage, G. A. Shipley, I. C. Smith, J. Schwarz, D. J. Ampleford, K. Beckwith, K. Peterson, J. L. Porter, G. A. Rochau, and D. B. Sinars, *Nucl. Fusion* **62**, 042015 (2021).
19. R. Battesti, J. Beard, S. Boser, N. Bruyant, D. Budker, S. A. Crooker, E. J. Daw, V. V. Flambaum, T. Inada, I. G. Irastorza, F. Karbstein, D. L. Kim, M. Kozlov, Z. Melhem, A. Phipps, P. Pugnat, G. Rikken, C. Rizzo, M. Schott, Y. Semertzidis, H. T. Ten Kate, and G. Zavattini, *Phys. Rep.* **765**, 1 (2018).
20. C. Vicario, A. Ovchinnikov, S. Ashitkov, M. Agranat, V. Fortov, and C. Hauri, *Opt. Lett.* **39**, 6632 (2014).
21. S. Weng, Q. Zhao, Z. Sheng, W. Yu, S. Luan, M. Chen, L. Yu, M. Murakami, W. B. Mori, and J. Zhang, *Optica* **4**, 1086 (2017).